Supplementary information

Improved electrochemical performance of solid-state lithium metal batteries with stable SEI and CEI layers via in situ formation technique

Tadesu Hailu Mengesha[a,b,c], Shimelis Lemma Beshahwured[a,b,d], Yola Bertilsya Hendri[a,b], Kumlachew Zelalem Walle[a,b], Yi-Shiuan Wu[a], Chun-Chen Yang[a,b,e*]

[a]Battery Research Center of Green Energy, Ming Chi University of Technology, New Taipei City 24301, Taiwan R.O.C.

[b]Department of Chemical Engineering, Ming Chi University of Technology, New Taipei City 24301, Taiwan, R.O.C.

[c]College of Natural and Computational Science, Department of Chemistry, Wolkite University, Wolkite, 07 SNNPR, Ethiopia.

[d]Department of Material Science and Engineering, Adama Science and Technology University, Adama, Ethiopia.

[e]Department of Chemical and Materials Engineering, and Green Technology Research Center, Chang Gung University, Taoyuan City 333, Taiwan, ROC

*Corresponding authors Tel.: +886 2 29089899 ext.4962/4952; fax: +886 2 29085941.
E–mail: ccyang@mail.mcut.edu.tw (C.-C. Yang)

1. Sandwich-type composite SSEs membrane synthesis

We synthesized sandwich-type solid polymer electrolyte membranes (SHSE1) with different constituents using solution casting. The first suspension comprised PVDF-HFP, LiTFSI, and SN (10 wt. % *versus* polymer) and 10 wt. % PDA@LALZO networked filler applied to build up the layer facing both the anode and cathode. The second suspension contained the same constituents as the first suspension, except 30 wt. % PDA@LALZO networked filler, which was used to construct the middle layer of the composite membrane. The weight ratio of PVDF-HFP to LiTFSI in each suspension was 2:1. DMF was used as a solvent to prepare the suspensions. We used a facile solution casting method to synthesize the SHSE membrane with a wet thickness of 150 μm (each side layer) and 500 μm (middle layer). The SHSE1 membrane was then dried in a vacuum oven at 60 °C for 24 h and peeled off the glass substrate. Further, the membrane was exposed to a cold-pressing hydraulic machine (1000 psi for 3 min) to reduce the thickness and enhance the packing density of the membrane and again dried in a vacuum oven at 80 °C for 12 h. Scheme 2 illustrates the synthesis of SHSE membrane using solution-casting method. For the control membrane (i.e., SHSE0), we used the same protocols but no PDA@LALZO filler from the anode side. The total thickness of the electrolyte membranes is controlled to *ca.*160 μm.

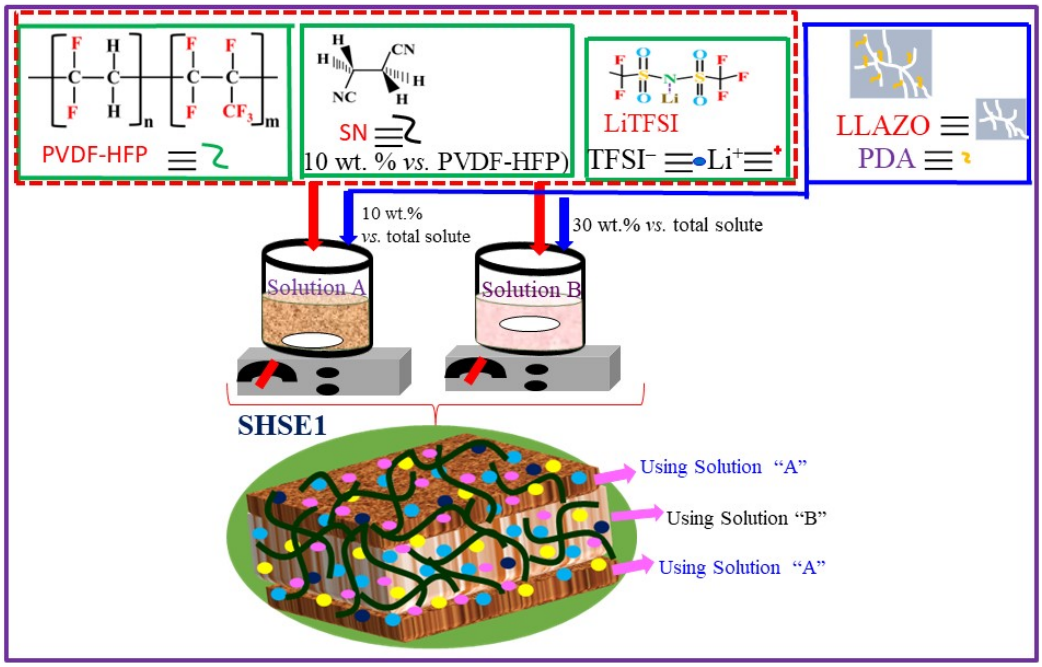

Scheme S1. A schematic representation of the synthesis procedure of SHSE1 composite membrane using a solution-casting method.

2. Surface modification of VGCF

In this study, we applied polydopamine (PDA) to modify the surface of VGCF to improve their wettability in matrices. First, we dissolved 2.3 wt. % of dopamine HCl in deionized (DI) water and then 1.4 wt. % of Tris-base to initiate self-polymerization. The VGCF was dispersed in DI water and ultrasonicated for 1 h in a separate beaker, followed by treatment with a PDA solution under continuous stirring overnight. Then, we collected the PDA-modified VGCF through centrifugation (6000 rpm with 10 min) and dried at 80 °C for 24 h. Hereafter, we refer to PDA-modified VGCF fillers as PDA@VGCF.

3. Synthesis of $LiNi_{0.8}Co_{0.1}Mn_{0.1}$ cathode material

$Ni_{0.8}Co_{0.1}Mn_{0.1}(OH)_2$ hydroxide precursor was fabricated *via* a facile co-precipitation approach, followed by a solid-state reaction with suitable annealing conditions. Typically, the required amount of nickel sulfate hexahydrate ($NiSO_4 \cdot 6H_2O$), cobalt sulfate heptahydrate ($CoSO_4.7H_2O$), and manganese sulfate monohydrate ($MnSO_4 \cdot H_2O$) were dissolved at 80:10:10 molar ratio. The required molar ratio of sodium hydroxide (4 M NaOH) and ammonium hydroxide (8 M NH_4OH) was separately dissolved in an aqueous medium container. Furthermore, the aqueous solution of transition metal sulfate, NaOH, and NH_4OH was injected into the Taylor-Couette Reactor (TCR). The reaction temperature of 60 °C and pH level of 11 was maintained throughout the reaction. After 10 h, the reactor attains a steady state. Then the reaction was completed, and the collected hydroxide precipitated product was washed with DI water and ethanol followed by dried off at 80 °C for 24 h. Finally, the obtained precursor powders and $LiOH.H_2O$ at a molar ratio of 1:1.05 were conducted in a solid-state reaction by using the dry ball mill method and then calcination at 830 °C for 12 h to form Bare-$LiNi_{0.8}Co_{0.1}Mn_{0.1}O_2$.

4. Preparation of lithiated-Nafion solution

Following the method developed by [1,2], we prepared Lithium Nafion (Li-Nf) by adding 25.2 mg of $LiOH \cdot H_2O$ into the commercial Nafion (5 wt. % in H_2O and 1-propanol, 10 mL) solution. The solution was then stirred at 60 °C for 2 h and dried in a vacuum oven at 80 °C for 12 h to afford lithiated Nafion (Li-Nf) residue. Then, 0.1 g of dried Li-Nf solid residue was dissolved and diluted in N-methyl pyrrolidone (NMP,

9.9 g), and the solution was stirred for 6 h to obtain a 1 wt.% Li-Nf solution (i.e., 1 wt. % in NMP).

5. Surface modification of NCM811 active materials by Li-Nf coating

Firstly, we dissolved 1 wt. % of as-prepared Li-Nf solid residue in NMP (N-Methyl-2-pyrrolidone, Sigma- Aldrich) and stirred until completely dissolved (*ca*. 3 h). Then we poured it slowly into another beaker containing pre-dispersed (*ca.*1 h) NCM811 cathode material suspension and continuously stirred for 12 h. Lastly, the as-coated NCM811 powder was filtered and dried in a vacuum oven for 12 h at a temperature of 60 ^{o}C (hereafter, we denoted as Li-Nf@NCM811). Lithium Nafion, which is a lithiated sulfonated tetrafluoroethylene-based fluoropolymercopolymer–has good ionic conductivity, high chemical stability, and serves as a protective layer on the cathode material. With these properties, Li-Nf can help to minimize the microcracks by covering the NCM811 particles and inhibit the surface reactions [3]. Fig. S4(a) presents the SEM images of Li-Nf@NCM811 powder. Further confirmation of Li-Nf layer production on NCM811 particles was achieved by performing XPS-based characterization of the NCM811 particles, as shown in Figs. S4(c) and (d). In detail, no peaks of F 1s can be observed in pristine NCM811, suggesting the absence of Li-Nf layer, as shown in Fig. S4(c). However, the F 1s spectra of Li-Nf@NCM811 is deconvoluted into two peaks at ~690.2 and 687.4 eV, which can be assigned to the C–F and Li–F bonds, respectively, as shown in Fig. S4(d). Similarly, the S 2p peak is observed on the Li-Nf coated NCM811 at 163.4 eV, while the corresponding peak is absent in the pristine sample, as shown in Fig. S4(c).

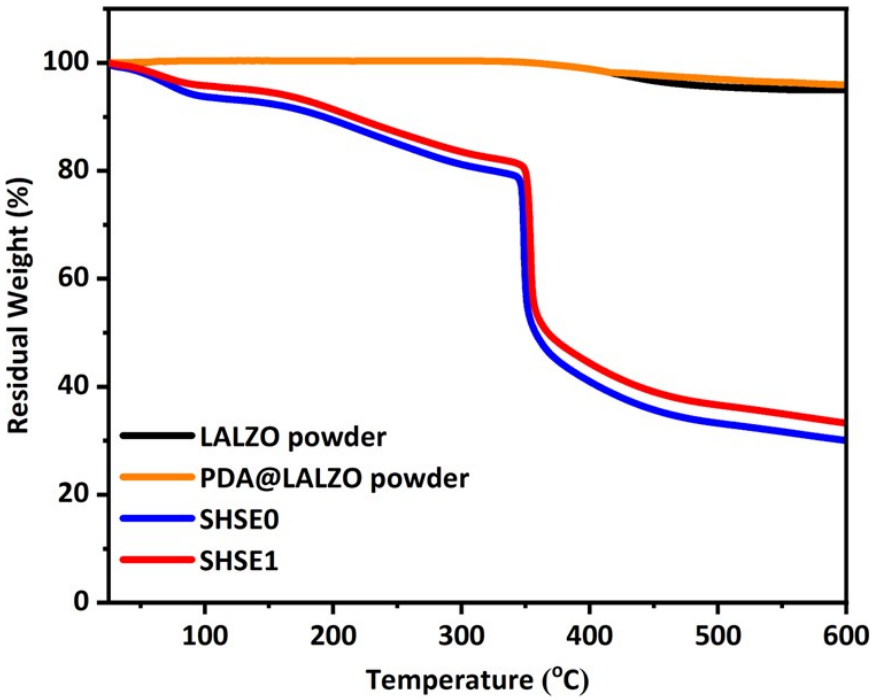

Fig. S1 TGA behavior of LALZO and PDA@LALZO fillers, SHSE0, and SHSE1 membranes

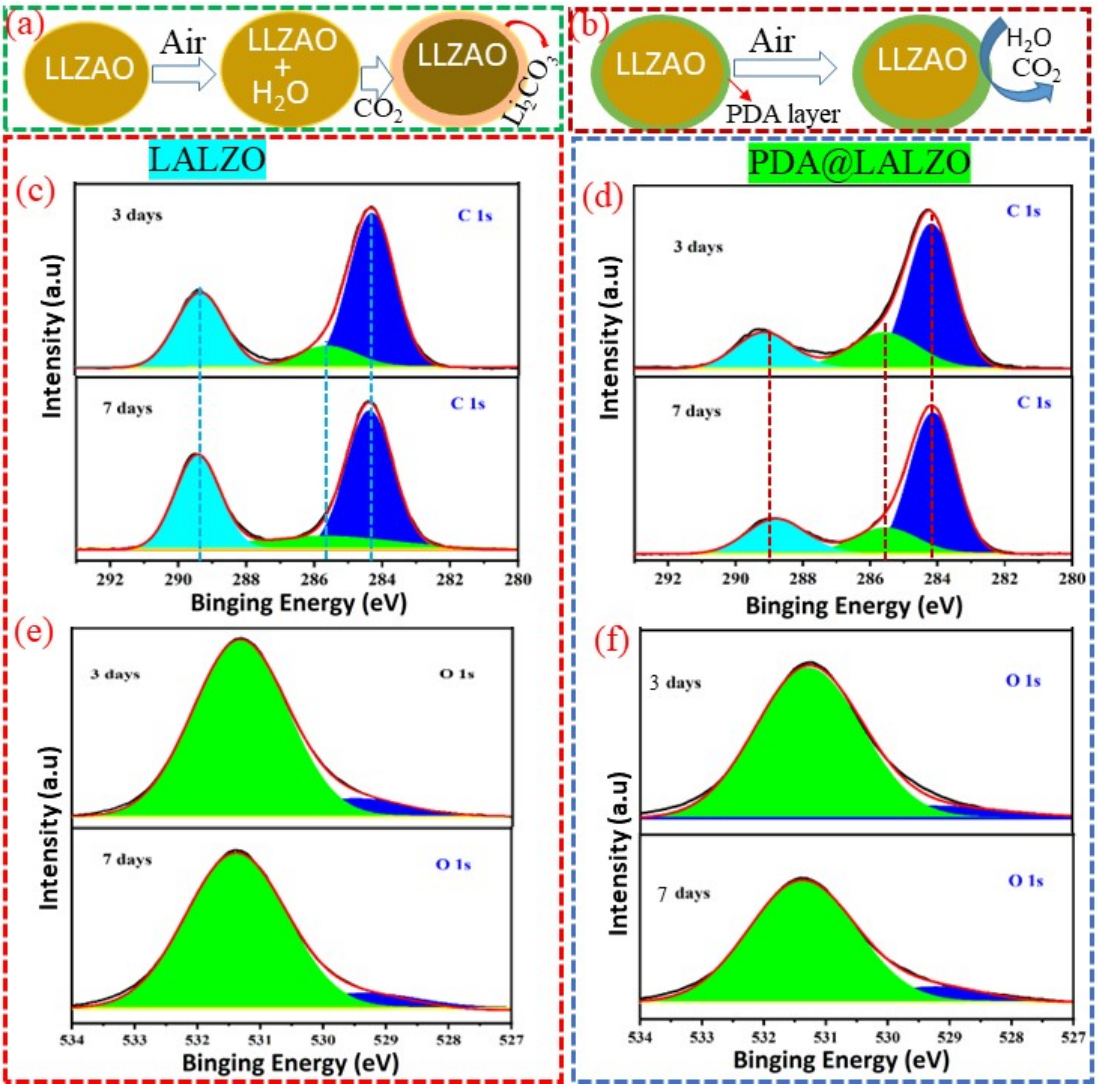

Fig. S2 Schematic presentation of (a). the possible interaction of LALZO with moisture; (b). application of PDA coating layer on minimizing the interaction of LALZO filler and moisture; (c)-(f). XPS spectra of aged LALZO and PDA@LALZO interconnected fillers.

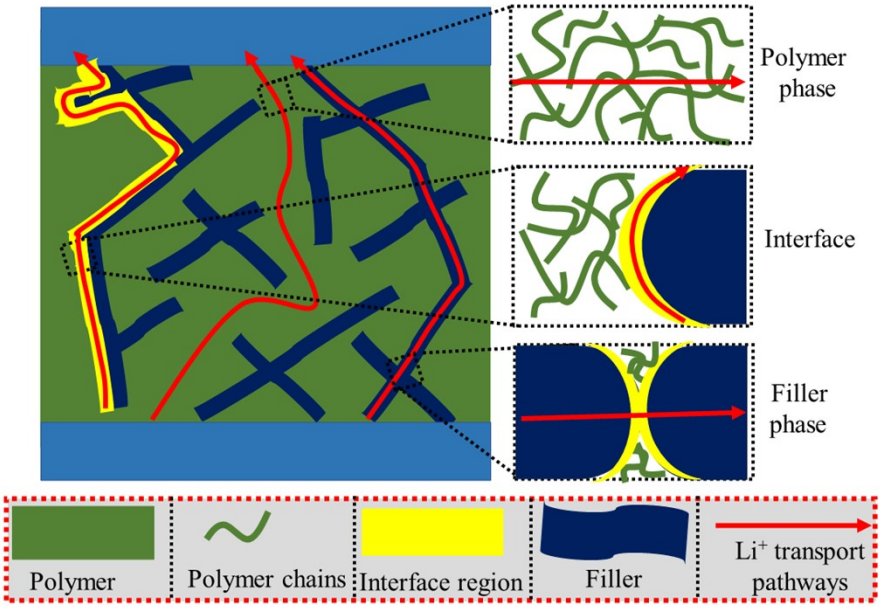

Scheme. S2 possible Li^+ migration pathways in the as-prepared composite solid electrolyte membranes.

Table S1 Quantification result (%) of ^6Li ss-NMR resonance spectra in different components of the as-prepared composite membranes before and after galvanostatic cycling.

Composite membranes	Before Cycling			After Cycling			
	LiTFSI	Interface	Filler	LiTFSI	Interface	Filler + interface	Filler
SHSE0	57.81	42.19	—	51.24	9.17	39.59	—
SHSE1	52.71	32.74	14.55	32.95	34.45	—	32.60

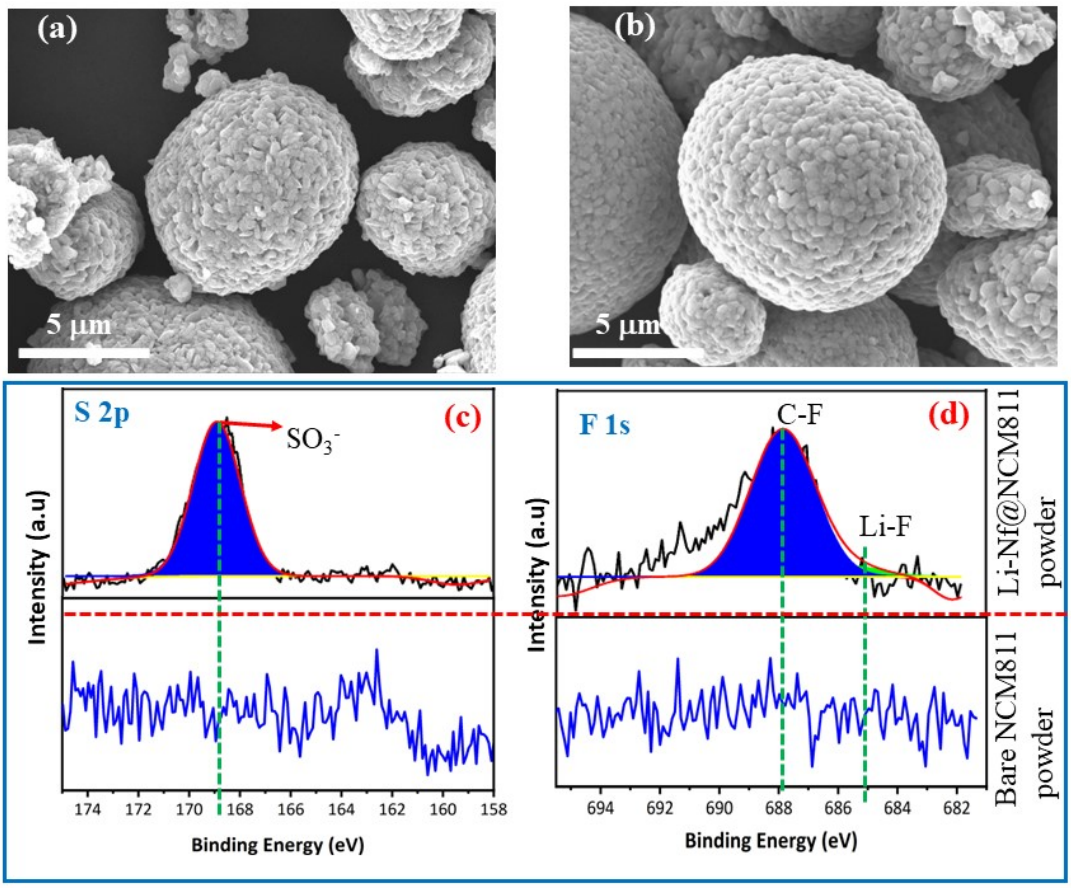

Fig. S3 SEM image of (a). bare NCM811, and (b). Li-Nf@NCM811; XPS spectra of bare and Li-Nf modified NCM 811 powders, (c). S 2p and (d) F 1s.

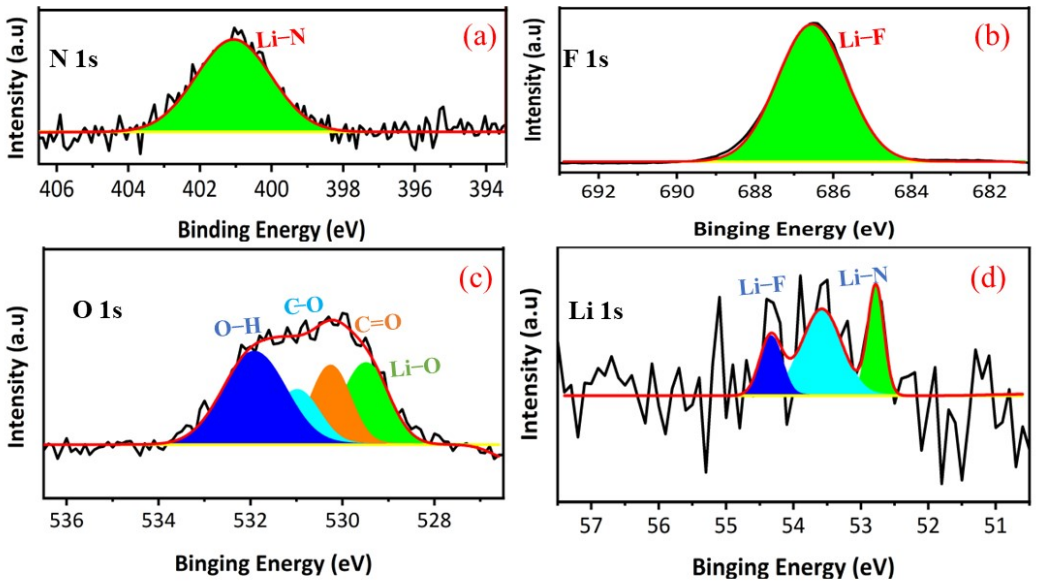

Fig. S4 XPS profile of (a). N 1s, (b). F 1s, (c). O 1s, and (d). Li 1s in modified lithium-metal surface.

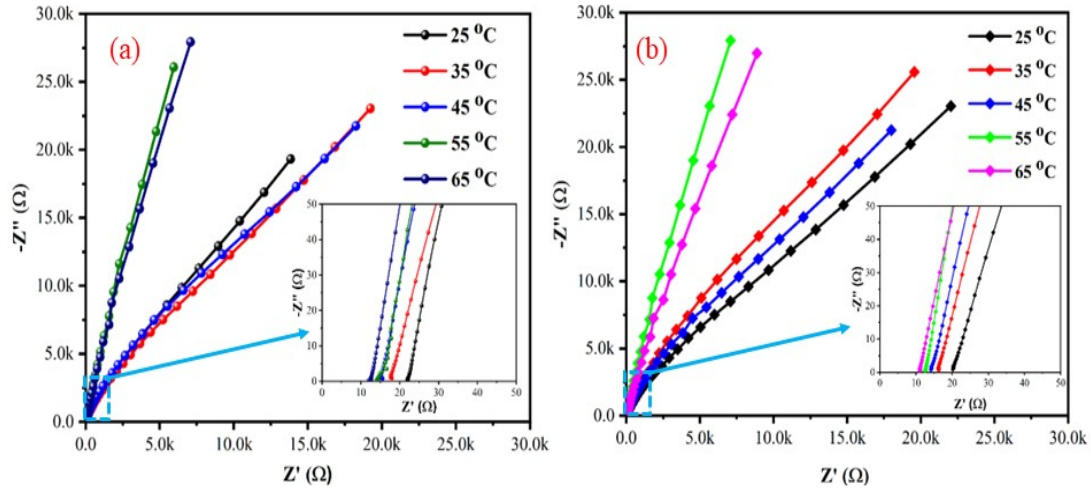

Fig. S5 EIS profiles of (a). SHSE0; (b). SHSE1 composite membrane measured at 25-65 °C.

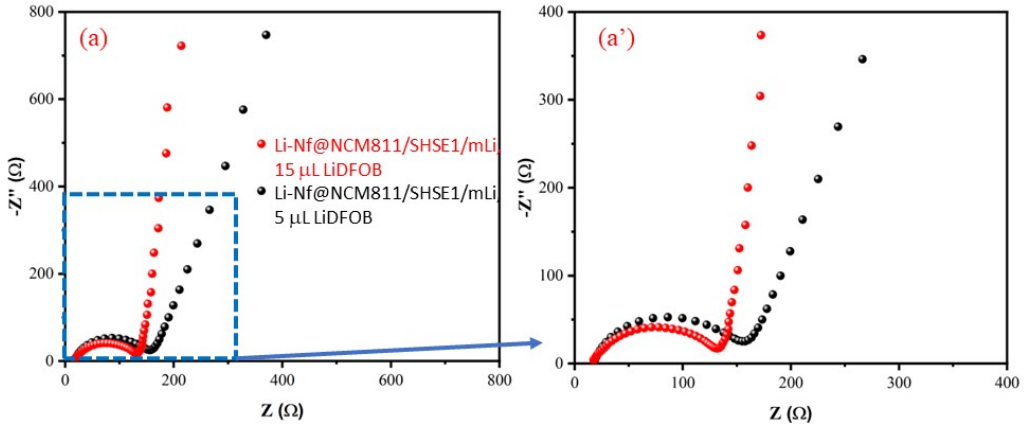

Fig. S6 EIS profile of Li-Nf@NCM811/SHSE1/mLi using 5 and 15 µL of LiDFOB-based liquid electrolyte.

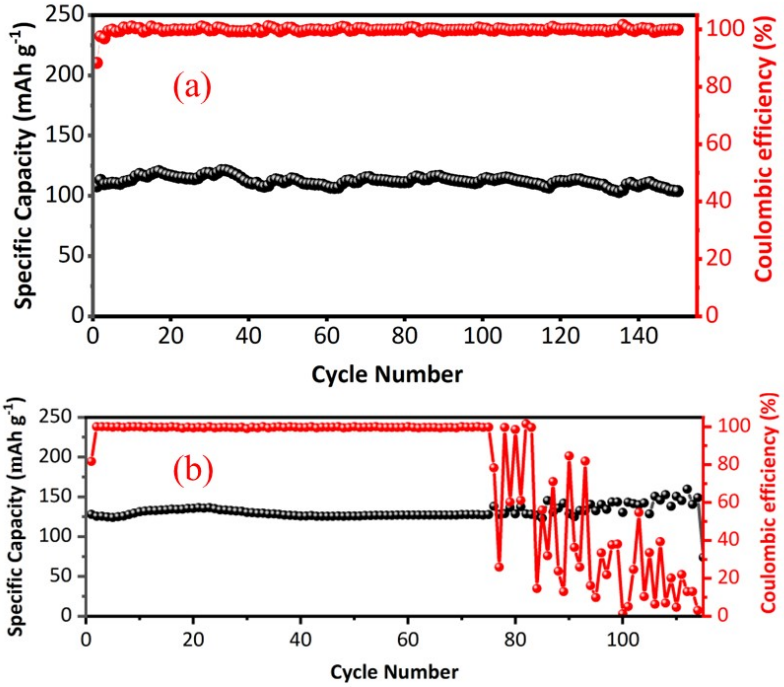

Fig. S7 The long-term cycling performance of Li-Nf@NCM811/SHSE1/mLi with 5 and15 µL of LiDFOB-based LE between 2.8-4.3 V at 1C/1C and at RT.

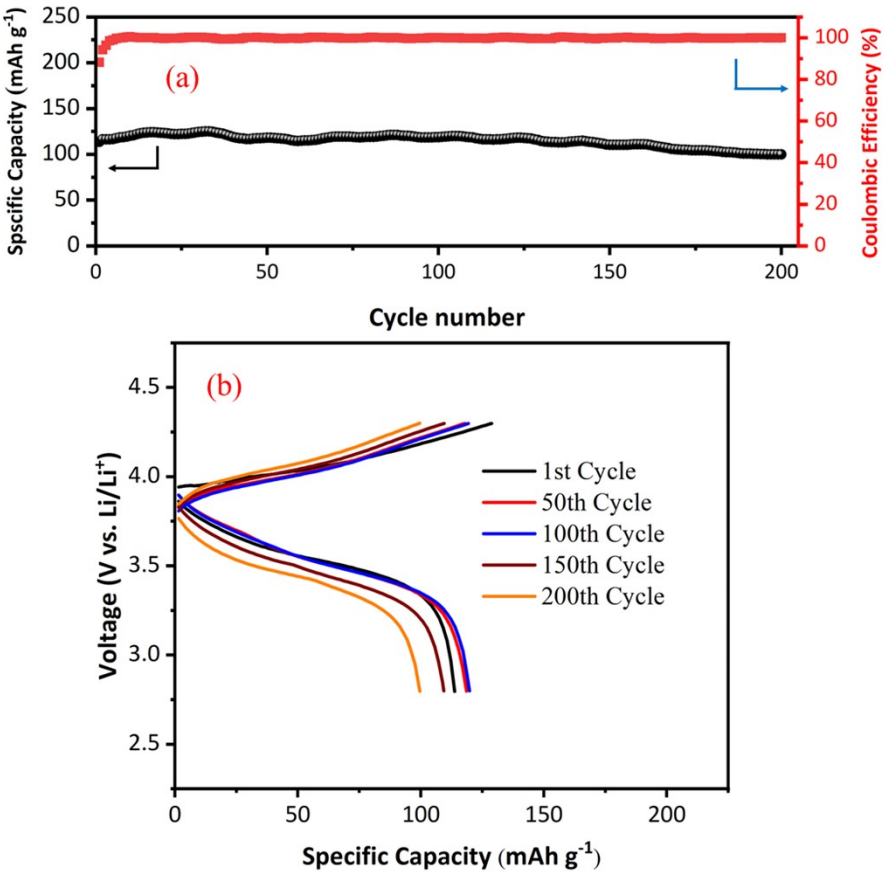

Fig. S8(a). The long-term cycling and (b). charge-discharge performance of Li-Nf@NCM811/SHSE1/mLi cell without LiDFOB-based LE added between 2.8-4.3 V at 1C and RT.

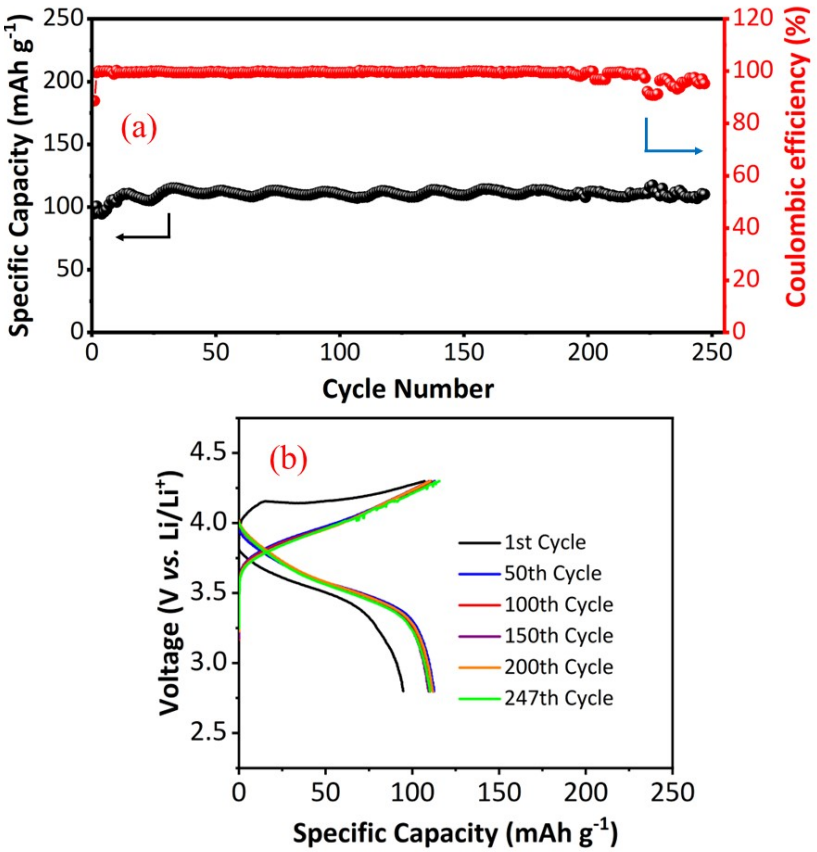

Fig. S9 (a). The long-term cycling and (b). charge-discharge performance of Li-Nf@NCM811/SHSE1/bLi with LiDFOB-based LE added between 2.8-4.3 V at 1C and RT.

Table S2 Summary of different resistance values of SHSE0 and SHSE1 membranes sandwiched between Li-Nf@NCM811-based cathode and mLi-metal anodes.

Cell configuration (Li-Nf@NCM811//mLi	Before cycle impedance values (Ω)				After cycle impedance values (Ω)				
	R_b	$R_{(a,i)}$	$R_{(c,i)}$	R_{total}	R_b	$R_{(a,i)}$	$R_{(c,i)}$	$R_{(ct)}$	R_{total}
SHSE1	11.97	7.22	91.24	110.43	38.28	2.63	101.68	156.90	299.49

SHSE0	12.17	23.27	92.37	127.81	46.84	2.17	114.80	193.50	357.31

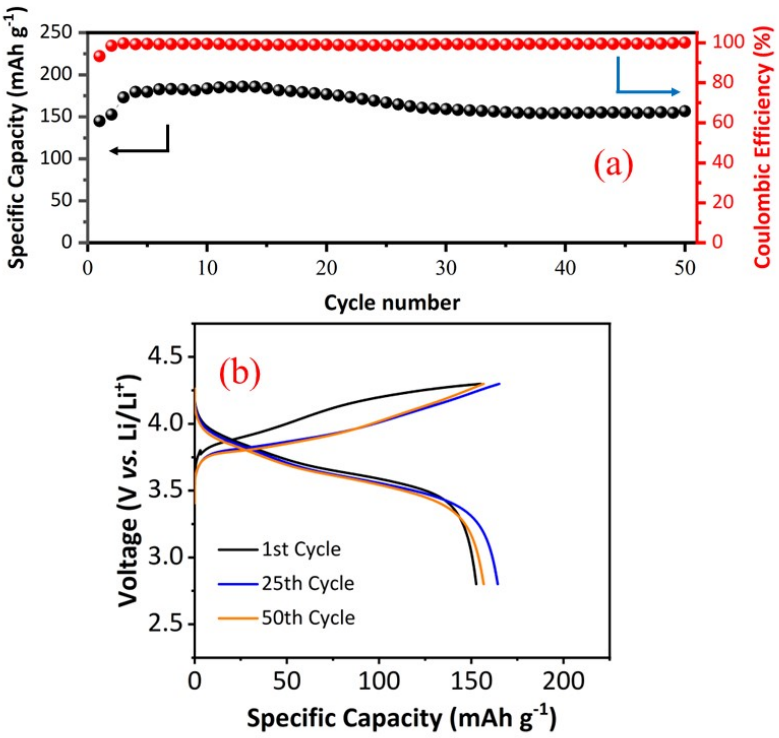

Fig. S10(a). Cycling profile, (b). the charge-discharge curve of 3 × 5 cm^2 pouch-type Li-Nf@NCM811/SHSE1/mLi cell at 0.1C between 2.8-4.3 V at RT.

Table S3 Comparative study of the characteristic performances of the current solid-state-based cells with related works performed elsewhere.

Data / Cells	Ionic conductivity (S cm^{-1}, °C)	CCD (mA cm^{-2}	Capacity (mAh g^{-1}) (cycles, °C)	Capacity retention (%)	Potential range (V), (C-rate)	Refs.
LFP/LLZTO-HMP/Li	7.3×10^{-4}, RT	1.91	138.6 (500, 25)	89.50	2.5–4.0 (0.2)	[3]
NCM622|B, F-CSE|Li	2.16×10^{-4}, 25	NA	143.8 (300, RT)	94.40	4.3–4.4 (1)	[4]
NCM622-8NCTs/SPE/Li	7.9×10^{-5}, 25	NA	90(100, 25)	69.23	2.7-4.2(1)	[5]
LFP/ PHTL-FEC-LLZTO/Li	6.52×10^{-5}, 50	NA	117.60 (200, 50)	88.5	2.8–4.1 (0.5)	[6]
NCM523| PEO-LLZTO@Aro| Li	4.57×10^{-4}, 20	1.4	NM (50, 50)	NA	2.8–4.3 (0.1)	[7]
Li-Nf@NCM811/ SHSE1/Li, coin cell	**5.47×10^{-4}, RT**	**2.5**	**108.85 (450, RT)**	**80.16**	**2.8–4.3 (1)**	**This work**
			109.20 (400, RT)	**78.01**	**2.8–4.3 (2)**	
Li-Nf@NCM811/ SHSE1/Li, 5×3 cm^2 pouch cell			**158.66 (50, RT)**	**83.00**	**2.8–4.3 (0.1)**	

FEC = fluoroethylene carbonate; a boron, fluorine-donating liquid electrolyte (B, F-LE); HMP = high-speed mechanical polishing, NA = not available

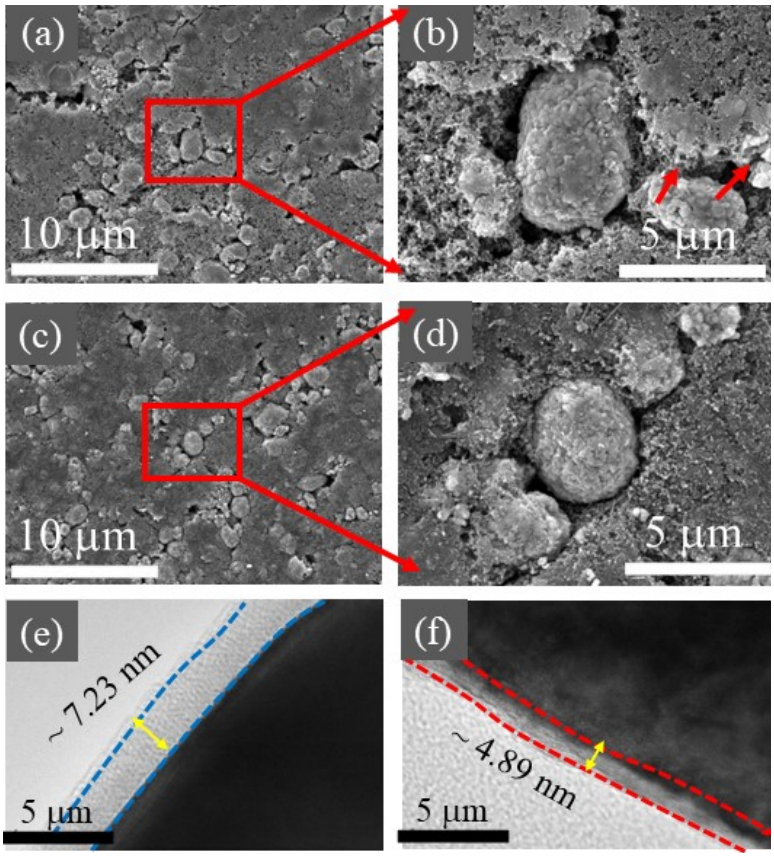

Fig. S11 SEM images of Li-Nf@NCM811 surface disassembled from coin-type cells cycled (a) and (b) without, and (c) and (d) with the addition of 10 μL LiDFOB LE; HR-TEM images of Li-Nf@NCM811 electrode cycled (e) and without (f) with the addition of LiDFOB-based LE.

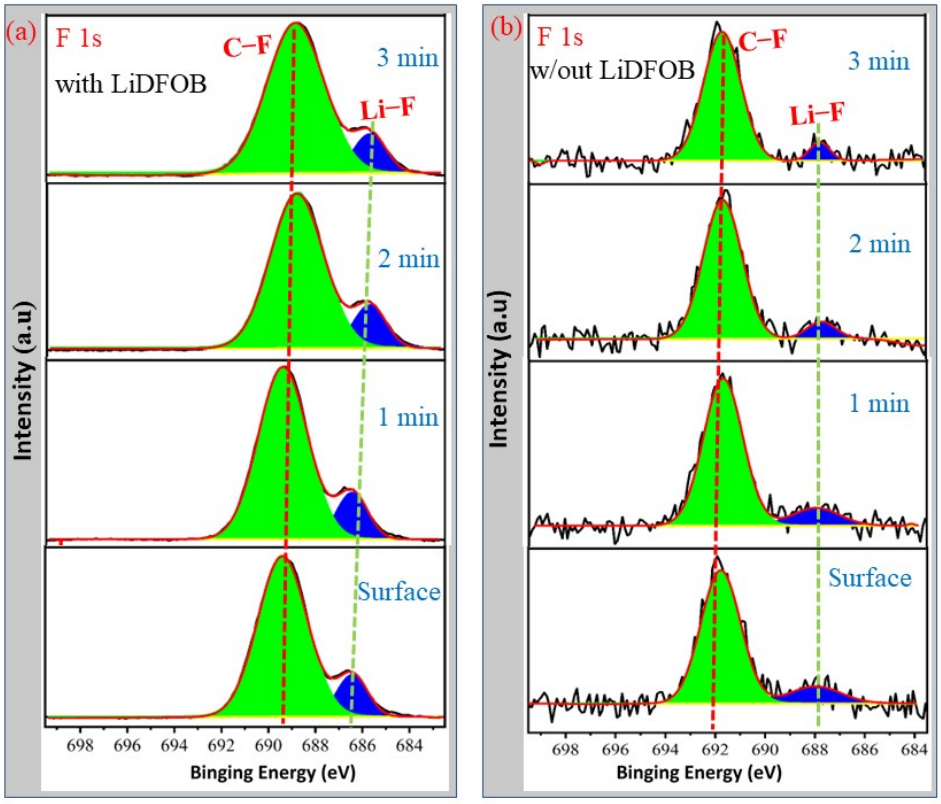

Fig. S12 XPS spectra of F 1s in cycled mLi-metal anodes: (a). with, and (b). without LiDFOB-based LE.

References

1 S. Jiang, Y. Lu, Y. Lu, M. Han, H. Li, Z. Tao, Z. Niu and J. Chen, *Chem. - An Asian J.*, 2018, **13**, 1379–1385.

2 K. Z. Walle, Y. S. Wu, S. H. Wu, J. K. Chang, R. Jose and C. C. Yang, *ACS Appl. Mater. Interfaces*, 2022, **14**, 15259–15274.

3 Z. Bi, N. Zhao, L. Ma, Z. Fu, F. Xu and C. Wang, *Chem. Eng. J.*, 2020, **387**, 124089.

4 X. Li, L. Cong, S. Ma, S. Shi, Y. Li, S. Li, S. Chen, C. Zheng, L. Sun, Y. Liu and H. Xie, *Adv. Funct. Mater.*, 2021, **31**, 1–10.

5 A. Orue, J. M. López del Amo, F. Aguesse, M. Casas-Cabanas and P. López-Aranguren, *Energy Storage Mater.*, 2023, **54**, 524–532.

6 Q. Wang, Y. Su, W. Zhu, Z. Li, D. Zhang, H. Wang, H. Sun, B. Wang, D. Zhou and L. Z. Fan, *Electrochim. Acta*, 2023, **446**, 142063.

7 J. Li, H. Zhang, Y. Cui, H. Da, Y. Cai and S. Zhang, *Chem. Eng. J.*, 2022, **450**, 138457.